

# Effect of Fluid Viscosity on Combined Free Forced Convection Flow Phenomena in Vertical Pipes

HOWARD L. GREENE and GEORGE F. SCHEELE

Cornell University, Ithaca, New York

Distorted velocity and temperature profiles are measured at low Reynolds numbers for upflow constant flux heating of water and two viscous Newtonian sucrose solutions in a long vertical pipe. Heated  $L/D$ 's ranged from 29 to 251. Experimental profiles at  $L/D = 251$  show general agreement with the fully developed profile theory based on natural convection effects, but additional profile distortion, attributed at least in part to radial viscosity variation with temperature, is observed even with water.

Natural convection induced transition to disturbed flow occurs for all three liquids as the ratio of heat input to flow rate is increased. The transition process involves the growth in amplitude and radial spread of initially small disturbances. Transition conditions and the dimensionless radial location of the first detectable instability are related to features of the distorted flow fields.

Physical property variations with temperature cause distortion of the fully developed parabolic velocity profile for laminar nonisothermal flow of a Newtonian fluid in a circular pipe. If the profile distortion is sufficiently great, flow instability may produce transition to fluctuating flow at very low Reynolds numbers. This transition has been investigated experimentally in vertical pipes for constant flux heating and cooling of water (3, 6, 9, 16, 17) and constant wall temperature heating and cooling of water (8, 17) and it has also been observed for constant flux heating of air (2). Metais and Eckert (10) summarize much of this work and attempt to incorporate the combined free and forced convection transition phenomenon within the overall context of forced, mixed, and free convection regimes for heated pipe flows. Such an approach is of qualitative value, but individual results may deviate greatly from the generalized correlation because of significant differences in hydrodynamic entry length prior to heating, radial position of probe at transition, probe diameter, pipe diameter, mode of heating, and direction of forced flow, which are not parameters of the correlation.

Theoretical analyses of the problem of flow field distortion with constant heat flux assumed have been presented for several cases. For the case where the fluid is Newtonian and only the density appearing in the gravity term of the equations of motion varies with temperature, it has been shown (3, 6, 8, 11, 12) that analytical solutions exist for the invariant fully developed velocity and temperature fields which are ultimately established in a long heat transfer section. In this case the maximum profile distortion occurs in the fully developed region and is a function only of the Grashof to Reynolds number ratio  $N_{Gr}/N_{Re}$  (or the Rayleigh number  $N_{Ra}$ ) and the direction of natural convection relative to the forced flow. Additional solutions have recently been obtained (4) based on power law behavior of the fluid.

Dye experiments have shown that the flow field dis-

tortion obtained for nonisothermal flow of water in a vertical tube is caused primarily by natural convection effects (8, 17), and measurements of essentially fully developed temperature profiles (3), and Nusselt numbers (16) have shown reasonably good agreement with the variable density constant heat flux theory when water is the fluid. Furthermore, constant flux transition data show a constant critical value of  $N_{Gr}/N_{Re}$  independent of  $N_{Re}$  for long heated pipes (16). Since transition is most likely associated with velocity profile instability, such data suggest the profiles approach a fully developed shape which remains invariant with further heated length; otherwise, for a given  $N_{Gr}/N_{Re}$ , a longer heated section would lead to greater profile distortion, so that the transition value of  $N_{Gr}/N_{Re}$  would continually decrease with increasing heated  $L/D$ .

Recently, Lawrence and Chato (9) have presented a numerical solution based on finite difference techniques for the velocity and temperature profiles when both radial density and viscosity variations are important. The profiles continue to develop, even at very large  $L/D$ , and never reach an invariant form. Center-line velocities measured by Lawrence and Chato for water flowing upward in a vertical heated tube show excellent agreement with the constant flux theory over the range of  $L/D$ 's studied and verify the possibility of profile distortion greater than that predicted by the constant viscosity theory.

The apparent discrepancy between those water experiments which suggest attainment of a fully developed flow and those which indicate a continually developing flow even in long heat transfer sections may arise because of the much larger radial temperature gradients and hence viscosity gradients present in the latter experiments. The analysis of Lawrence and Chato is consistent with this interpretation but cannot be used to substantiate the apparently fully developed data of other investigators because the flow fields entering the heated sections do not correspond to the uniform velocity distribution assumed in the theory. On the other hand, there may be no discrepancy, for it is not certain that the flow has been truly fully developed in any experiments because agreement between experimental and theoretical fully developed tem-

Howard L. Greene is at The University of Akron, Akron, Ohio.

perature profiles and in particular Nusselt numbers prior to transition is not a sensitive test of the theory. While a change in the Grashof to Reynolds number ratio can produce a significant change in the shape of the theoretical velocity distribution, as shown by the theoretical curves in Figure 3 for constant flux upflow heating (the case to be considered in this paper), corresponding changes in the theoretical temperature profiles are less pronounced as shown in Figure 6.

It is important to know if, under conditions of heating and flow, carefully chosen to minimize viscosity variation effects, the velocity profiles attained at large  $L/D$  can actually become essentially invariant so as to be predictable from the constant viscosity theory because the results of these experiments have been used to draw fundamental conclusions about the stability of distorted flow fields. Such experiments presumably satisfy the desirable conditions for experimentally evaluating pipe flow stability theories, namely a region where the flow profile is invariant (which makes it possible to determine which profile is responsible for the initial instability) and a theory for predicting the equation of the invariant profile. For example, the experiments of Scheele and Hanratty (16) for upflow constant flux heating indicate that pipe flow is unstable to small disturbances only for  $N_{Gr}/N_{Re}$  ratios which characterize theoretical constant viscosity velocity profiles having a point of inflection, a result which disagrees with inviscid stability predictions based on rotationally symmetric disturbances (13) but which may be in agreement with recently developed non-symmetric disturbance theories (1, 14). Similarly, Scheele and Greene (15) have used constant flux results together with the constant viscosity theory to evaluate finite disturbance transition theories.

This paper examines the adequacy of the constant viscosity theoretical Newtonian analysis for constant flux upflow heating of water by presenting velocity and temperature profiles measured simultaneously for conditions where fully developed flow has been observed previously. Measurement of the distorted velocity profiles, which has never before been done, should be the most valid test of the analytical solutions and the conditions leading to instability. The adequacy of the analysis is then investigated for two aqueous sucrose solutions, which makes it possible to study the effect of significantly larger radial viscosity variations, and the first transition data resulting from flow field distortion for liquids more viscous than water are presented.

## EXPERIMENTS

The experimental apparatus, shown in Figure 1, consisted of a 29 ft. vertical length of 1.025-in. I.D. copper pipe which was inserted at the lower end into the pressure feed tank and connected at the top, through a calibrated rotameter, to the collector tank. A 21½ ft. section of the test pipe was electrically insulated and wrapped with chromel heating ribbon in such a way that the heated length could be varied from 2½ to 21½ ft. and the heat inputs from 0 to 40 w./ft. of pipe. The pipe inside diameter represented a compromise between the small diameters necessary to obtain large heated  $L/D$ 's in the limited available space and the large diameters desirable for minimizing radial temperature gradients and hence variable viscosity effects.

Runs were made by applying 16 to 20 lb./sq.in. air gauge pressure to the feed tank, forcing fluid up through the test pipe. The heated length, heat flux, and flow rate were set at the desired values and the system allowed to attain steady state, which was indicated by constancy of the outlet temperature. The liquids used were water, 45 wt. % sucrose in water with a viscosity of 8.4 centipoise at 25°C., and 55 wt. % sucrose in water with a viscosity of 21.5 centipoise at 25°C.

All liquid properties were evaluated at outlet conditions for calculating Reynolds and Grashof numbers.

Heat distorted velocity profiles across the pipe diameter were measured with a movable impact tube constructed from 1/16-in. I.D. by 3/32-in. O.D. stainless steel hypodermic tubing which was located at the outlet end of the heated section. A static pressure tube was attached to the pipe wall at a point horizontally adjacent to the impact tube. The static and impact tubes were both connected to a specially designed differential micromanometer which has been described previously (5). Accurate velocity profiles could be obtained only for water because of the poor response of the micromanometer to the more viscous liquids. Point fluid temperatures were simultaneously obtained by using a 0.014-in. diameter bead thermistor mounted coaxially at the tip of the impact tube. Transition to disturbed flow was detected by observing temperature fluctuations in the flow field. This method of determining transition is supported by results of Lawrence and Chato (9), who found temperature fluctuations to be a sensitive indicator of the onset of laminar instability.

## THEORY

Distorted laminar flow velocity and temperature profiles resulting from natural convection effects for heated pipe flows of Newtonian liquids have been described mathematically (3, 6, 8, 11, 12) by combining the appropriate forms of the momentum and energy equations and assuming fluid density variation only in the buoyancy term of the momentum equation. For steady state constant flux heating in a vertical pipe of a Newtonian fluid whose vis-

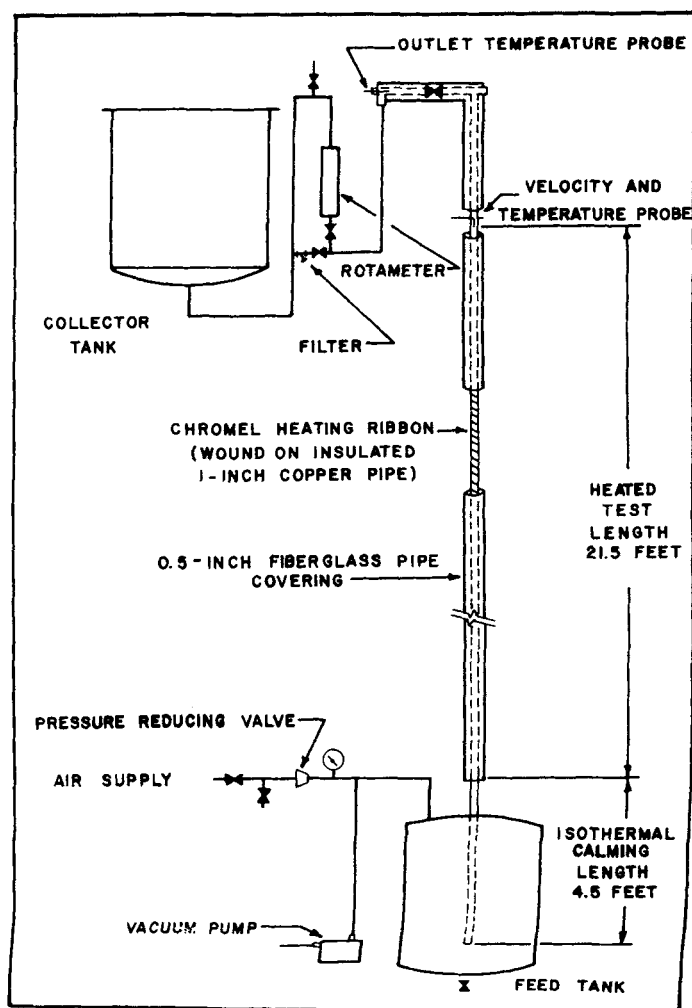


Fig. 1. Experimental apparatus.

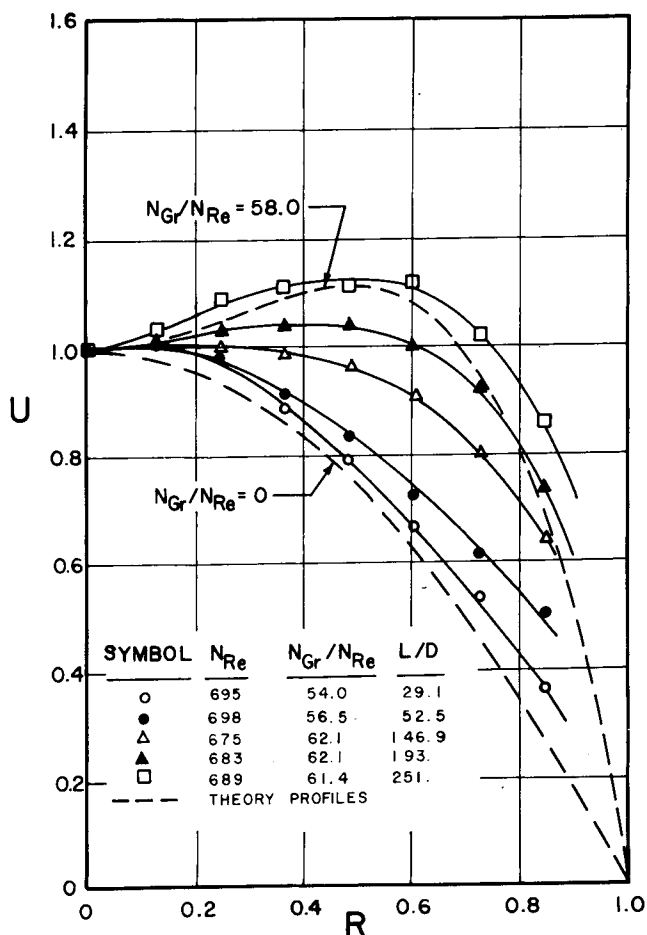


Fig. 2. Developing distorted velocity profiles for water.

cosity is assumed temperature independent, solutions for the distorted velocity and temperature profiles may be expressed as

$$U = \frac{u}{U_c} = \text{ber}(K^{1/4}R) + (g/f)\text{bei}(K^{1/4}R) \quad (1)$$

$$T = \frac{t_w - t}{t_w - t_c} = \frac{f \text{bei}(K^{1/4}R) - g \text{ber}(K^{1/4}R) - f \text{bei}(K^{1/4}) + g \text{ber}(K^{1/4})}{g \text{ber}(K^{1/4}) - g - f \text{bei}(K^{1/4})} \quad (2)$$

where

$$f = \frac{(K^{1/4}/2)\text{bei}(K^{1/4})}{\text{ber}'(K^{1/4})\text{ber}(K^{1/4}) + \text{bei}'(K^{1/4})\text{bei}(K^{1/4})} \quad (3a)$$

$$g = \frac{-f \text{ber}(K^{1/4})}{\text{bei}(K^{1/4})} \quad (3b)$$

$$K = \frac{2N_{Gr}}{N_{Re}} \quad (3c)$$

A more sensitive comparison of theoretical with experimental temperature profiles can be made by considering the temperature difference  $t - t_c$  which is predicted theoretically by

$$t - t_c = \left( \frac{2}{N_{Gr}/N_{Re}} \right)^{1/2} \left( \frac{qa}{k} \right) (f \text{bei}(K^{1/4}R) + g - g \text{ber}(K^{1/4}R)) \quad (4)$$

While the dimensional profiles must agree at both the center and the wall, values of  $t - t_c$  are forced to agree only at the center. Furthermore, only the probe thermistor need be used to obtain experimental values, eliminating any possible discrepancy arising from a systematic error between the probe and wall thermistors.

Solutions to Equations (1) and (4) are shown in Figures 3 and 7, respectively, for representative values of  $N_{Gr}/N_{Re}$  and are valid for positive  $K$ , that is, for upflow heating of a fluid with a positive coefficient of volumetric expansion.

## RESULTS AND DISCUSSION

### Velocity Profiles

Experimental velocity profiles were measured for water only. The data are presented as the ratio of local to centerline velocity  $u/U_c$  because this parameter is most readily calculated from the micromanometer readings. Measurements of fully developed isothermal velocity profiles were made to test the velocity determinations. These results indicate that measured velocity ratios are accurate to within about 6% only for dimensionless radii less than 0.80 because of the large probe diameter used. Similar accuracy is assumed in analysis of the distorted profiles. The usefulness of the micromanometer was further limited in that precise readings could be obtained with water only for  $N_{Re} > 400$  because of the second order dependence of impact pressure on fluid velocity.

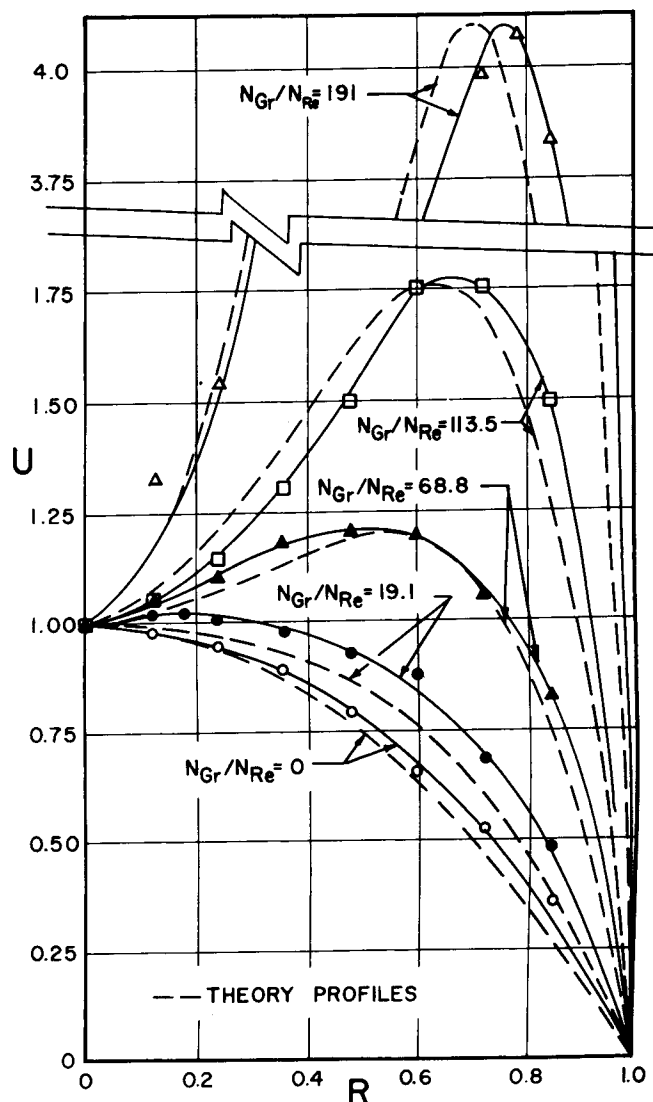


Fig. 3. Distorted velocity profiles for water at  $L/D = 251$ .

A series of developing profiles at constant  $N_{Gr}/N_{Re} = 60$  and  $N_{Re} = 680$  is plotted in Figure 2 along with the comparable theoretical isothermal and fully developed profiles. The hydrodynamic entry length preceding the heated section increases from a minimum of 53 pipe diam. as the heated length decreases, so that for Reynolds numbers less than 900 the flow entering the heated section should be fully developed for all heated lengths. As expected, distortion of the initially parabolic profile increases with heated length. At  $L/D = 251$ , the maximum obtainable in the present equipment, the experimental profile shows good agreement with the theoretically predicted fully developed one. The fact that the profile shape is still changing between  $L/D = 193$  and  $L/D = 251$  indicates that the length necessary for fully developed flow may be in excess of 251 pipe diam.

Figure 3 shows a typical series of velocity profiles measured at  $L/D = 251$  for a radius Reynolds number of 530. The profile distortion increases with increasing  $N_{Gr}/N_{Re}$ , as predicted by theory. While the agreement with theory is quite good over the range of  $N_{Gr}/N_{Re}$  studied, indicating that profile distortion results primarily from natural convection effects, the experimental profiles differ from the theoretical ones in one important respect. A radial shift in the location of  $U_{max}$  is already observed at  $N_{Gr}/N_{Re} = 19.1$ , while theory predicts no shift until  $N_{Gr}/N_{Re}$  exceeds 32.94. The shift is small but sufficiently pronounced that it cannot be attributed to experimental error in the velocity measurements, because the micromanometer construction is such that the radial location of  $U_{max}$  could be determined within  $R = 0.03$ . In addition, the shift occurs in a region near the center of the pipe, where probe-wall inter-

actions are minimal, and accuracy of measured velocity ratios is highest. It seems most likely that this radial shift in  $U_{max}$  is caused by radial viscosity variation with temperature, since a decrease in liquid viscosity with increasing temperature should further blunt the velocity distribution, reinforcing the distortion resulting from natural convection. Supporting this interpretation is the additional outward radial displacement of  $U_{max}$  from the theoretical predictions also observed at higher values of  $N_{Gr}/N_{Re}$ .

The radial viscosity variation also may be responsible for the continued profile development observed at large  $L/D$ , although the difference between wall and centerline temperature is less than  $4^\circ\text{C}$ . This possibility is considered in the next section.

#### Temperature Profiles

Temperature profiles were measured for both water and the viscous sucrose solutions. Representative developing profiles are shown in Figure 4 for water and Figure 5 for 45% sucrose. Again, the hydrodynamic entry length is adequate to ensure that the flow entering the heated section is fully developed in all cases. At small  $L/D$  the profiles are characterized by steep temperature gradients near the wall, while near isothermal conditions prevail in the central core of fluid. Both graphs show that to approach fully developed flow requires large heated lengths even at comparatively small Reynolds numbers. The water temperature profiles in Figure 4 were measured simultaneously with the velocity profiles in Figure 2 and confirm the result that profile development is still occurring between  $L/D = 193$  and  $L/D = 251$ , with the measured temperature difference  $t_w - t_c$  at  $L/D = 251$  nearly 20% below that predicted by theory. The deviation between

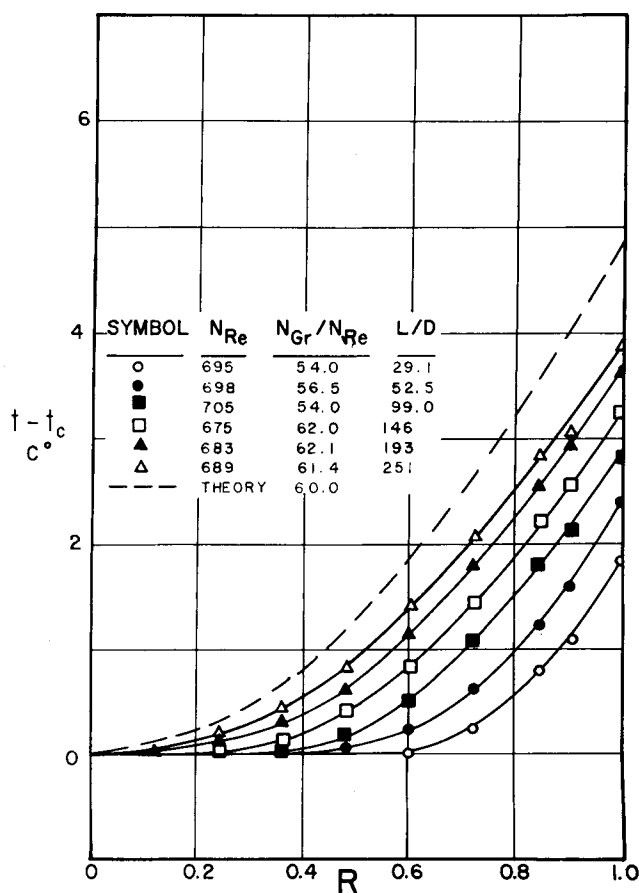


Fig. 4. Developing temperature profiles for water.

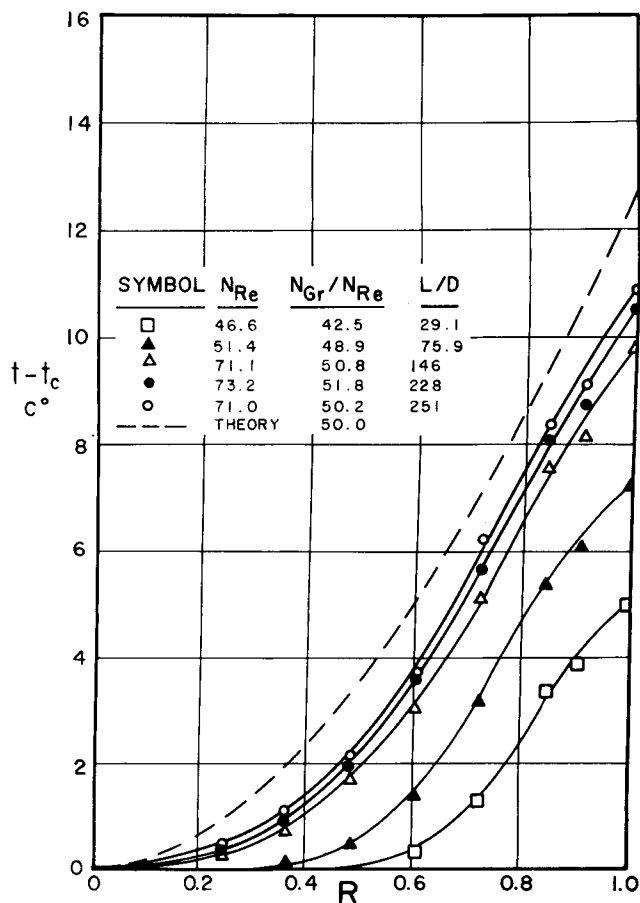


Fig. 5. Developing temperature profiles for 45% sucrose solutions.

the final sucrose profile and theory, shown in Figure 5, is similar to that obtained for water.

The observed deviation between theoretical and experimental temperature profiles at large  $L/D$  can be explained qualitatively on the basis either of insufficient heated  $L/D$  for complete profile development or of radial viscosity variations which reduce the resistance to flow of the hotter, less viscous fluid near the wall. If the latter effect is primarily responsible, the possibility of experimentally obtaining essentially invariant profiles for flow studies seems remote.

There is evidence to support the hypothesis of insufficient heated  $L/D$ . The developing length criterion of Hallman (7)

$$L/D = (0.04 \text{ to } 0.08) N_{Re} N_{Pr} \quad (5)$$

which neglects the possibility of continued development caused by viscosity variation, predicts a required  $L/D$  between 176 and 352 for water at  $N_{Re} = 680$  and between 152 and 304 for the 45% sucrose at  $N_{Re} = 50$ . The approximately equivalent approach of the experimental profiles to the corresponding fully developed theoretical ones for the two fluids is consistent with the use of the parameter  $N_{Re} N_{Pr}$  in Equation (5). The Prandtl number effect on development length predicted by the Hallman criterion means that fully developed flows for viscous fluids can be obtained only at low Reynolds numbers in long pipes. This fact suggested limiting maximum experimental radius Reynolds numbers for water and the 45 and 55% sucrose solutions to about 600, 95, and 25, respectively, in the present study, since  $N_{Pr}$  for each test solution did not vary significantly over the range of experimental conditions.

In downflow constant flux heating of water in a vertical pipe with heated  $L/D = 251$ , Williams (19) found that flow was fully developed only for Reynolds numbers less than approximately 200. Furthermore, he found that at these low flow rates the agreement between experiment and constant viscosity theory was excellent.

There is also evidence which indicates that radial viscosity variation is not the primary cause of the continuing temperature profile change observed even at large  $L/D$ . In the first place, the effect of a temperature dependent viscosity should be ultimately to decrease the magnitude of the radial temperature difference  $t_w - t_c$ , while the opposite effect is obtained experimentally. It is, of course, possible that in sufficiently long pipes the viscosity effect would finally predominate.

Furthermore, for a given liquid at a fixed Reynolds number, the percent deviation between experiment and theory shows little effect of increasing  $N_{Gr}/N_{Re}$ , even though the radial temperature gradient and hence viscosity variation is increased. This is shown in Figure 6 for two water runs whose values of  $t_w - t_c$  differ by a factor of 3. The unexpected curvature of the temperature profile near the wall seen in Figure 6 for the low  $N_{Gr}/N_{Re}$  ratio and in Figure 5 for small  $L/D$  ratios may result from the presence of the probe, since this is the region where velocity measurements were also found to be in error. However, recent experimental results obtained by Scheele (18) using a smaller 0.03 in. diameter probe confirm the existence of this profile deviation.

One final reason for concluding that insufficient heated length is primarily responsible for the continuing development of the temperature profiles is afforded by a comparison of results for the three different viscosity fluids studied. To make the comparison most meaningful, it is helpful to look first at the convection theory prediction of  $t_w - t_c$ , since it has already been shown that profile distortion is determined primarily by convection effects. When  $R =$

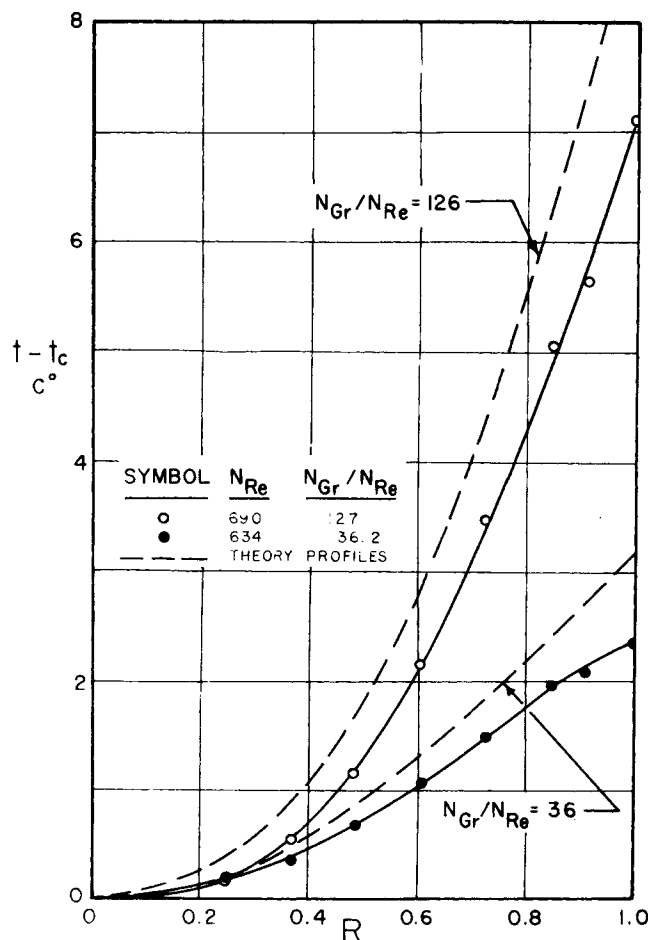


Fig. 6. Temperature profiles for water at  $L/D = 251$ .

1.0,  $t = t_w$ , and Equation (4) becomes

$$t_w - t_c = \left( \frac{2}{N_{Gr}/N_{Re}} \right)^{1/2} \left( \frac{qa}{k} \right) (f \operatorname{bei}(K^{1/4}) + g - g \operatorname{ber}(K^{1/4})) \quad (6)$$

From the definition of  $N_{Gr}/N_{Re}$  it can be shown that

$$\frac{qa}{k} = \left( \frac{N_{Gr}}{N_{Re}} \right) (N_{Re}) \left( \frac{\mu^2}{a^3 \rho^2 g \beta} \right) \quad (7)$$

so that

$$t_w - t_c = \left( \frac{N_{Gr}}{N_{Re}} \right)^{3/4} \left( \frac{N_{Re}}{2^{1/4}} \right) \left( \frac{\mu^2}{a^3 \rho^2 g \beta} \right) \psi \left( \frac{N_{Gr}}{N_{Re}} \right) \quad (8)$$

where

$$\psi \left( \frac{N_{Gr}}{N_{Re}} \right) = (f \operatorname{bei}(K^{1/4}) + g - g \operatorname{ber}(K^{1/4})) \quad (9)$$

For runs with different fluids at equivalent  $N_{Gr}/N_{Re}$  and where  $a$ ,  $\rho$ ,  $g$ , and  $\beta$  do not vary significantly

$$\frac{(t_w - t_c)_a}{(t_w - t_c)_b} \approx \left( \frac{N_{Re,a}}{N_{Re,b}} \right) \left( \frac{\mu_a^2}{\mu_b^2} \right) \quad (10)$$

where the subscripts refer to fluids (a) and (b).

Equation (10) shows that the effect of increasing radial temperature variations (and hence radial viscosity variations) for a given liquid at a fixed  $N_{Gr}/N_{Re}$  can be studied by increasing  $N_{Re}$ . However, if the Hallman development length criterion is even qualitatively correct, the extent to which  $N_{Re}$  can be increased while still maintaining fully developed flow in any reasonable size apparatus is limited. To obtain greater radial viscosity variations it is necessary

to use more viscous liquids, since at a given value of  $N_{Re}N_{Pr}$  (representing an equivalent approach to fully developed flow),  $t_w - t_c \propto \mu$ . This has been done in the present study by using two viscous aqueous sucrose solutions. At a given  $N_{Re}N_{Pr}$  and  $N_{Gr}/N_{Re}$ , experimental  $t_w - t_c$  values of 45 and 55% sucrose are about four and seven times that of water, respectively, while radial viscosity variations are 6.6 and 7.8 times as large.

If radial viscosity variations are primarily responsible for the continuing profile development, one would expect the approach to the fully developed constant viscosity profiles to be less with increasing liquid viscosity. Figures 4 and 5 show no such trend at  $L/D = 251$ . A similar result is obtained from the data presented in Figure 7, substantiating the conclusions that the lack of close agreement between experimental and theoretical temperature profiles is most likely caused by insufficient heated  $L/D$  at the higher Reynolds numbers studied.

#### Transition Conditions

The heat flux and flow conditions necessary to initiate detectable disturbances after 21½ ft. of heated pipe for the three fluids studied are shown in Figure 8, where the critical  $N_{Gr}/N_{Re}$  is plotted vs.  $N_{Re}$ . A few of the experimental results for water reported by Lawrence and Chato (9) and Scheele and Hanratty (16) are also plotted. The transition results of Brown (3), Hallman (6), and Scheele and Greene (15) are not conveniently shown here, since they were obtained at very low  $L/D$ , yielding critical  $N_{Gr}/N_{Re}$  values which are as much as one order of magnitude larger than those shown. Scheele and Hanratty (16) have shown that except in very long pipes the

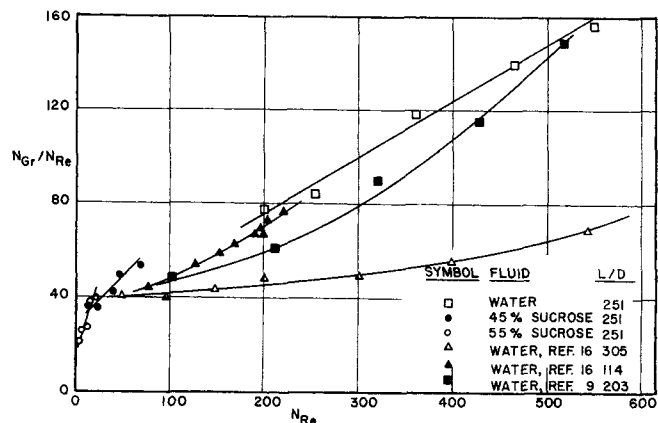


Fig. 8. Transition conditions for upflow heating.

critical  $N_{Gr}/N_{Re}$  is a strongly decreasing function of heated  $L/D$ .

The region below each line in Figure 8 represents stable laminar flow for the given fluid and heated  $L/D$ . The lines represent conditions just sufficient for transition, while the area above each line indicates conditions severe enough to generate observable flow field fluctuations in heated pipes with  $L/D$ 's less than given (251 in the present study).

The previous studies show a consistent trend, with the transition  $N_{Gr}/N_{Re}$  ratio decreasing with increasing heated  $L/D$  at a given  $N_{Re}$  until a limiting value is reached in long pipes. However, for water a comparison of the present results at  $L/D = 251$  with those of Lawrence and Chato at  $L/D = 203$  and Scheele and Hanratty at  $L/D = 114$  shows the opposite  $L/D$  effect. This apparent contradiction is most likely the result of differences in the experimental apparatus. The pipe diameters vary from 1.025 in. in the present study to 0.625 in. in the Scheele and Hanratty work for  $L/D = 114$  and to 0.424 in. in the Lawrence and Chato experiments. The radial temperature difference at a fixed  $N_{Gr}/N_{Re}$  and  $N_{Re}$ , which is proportional to  $a^{-3}$ , was thus approximately fourteen times larger in the Lawrence and Chato studies and 4.4 times larger in the Scheele and Hanratty experiments than in the present experiments, leading to much larger radial viscosity gradients, greater distortion of the flow field at a given  $N_{Gr}/N_{Re}$ , and, consequently, lower transition values of  $N_{Gr}/N_{Re}$  at a fixed  $N_{Re}$  and  $L/D$ . If this explanation is correct, the present studies should show the largest transition  $N_{Gr}/N_{Re}$  ratios for a given  $L/D$  because no other work has used as large a diameter pipe. It should also be pointed out that the fluid profile entering the heated section was flat in the Lawrence and Chato experiments and parabolic in the other studies, further complicating any comparison of the results. Only for similar entry conditions and pipe diameters is there likely to be a unique relationship between the transition value of  $N_{Gr}/N_{Re}$  and  $N_{Re}$  for a given  $L/D$ .

The results indicate that natural convection induced instabilities can cause transition not only for water flow but also for flow of more viscous fluids where variable viscosity effects are more important. The low Reynolds numbers necessary to obtain transition with the viscous sucrose solutions lead to the conclusion that in many practical situations disturbed flow conditions would not be encountered with viscous liquids. Scheele and Greene (15) have previously presented transition data which show the conditions necessary for disturbance growth for sucrose solutions in short heated pipes.

Each fluid shows an increase in the critical  $N_{Gr}/N_{Re}$  as

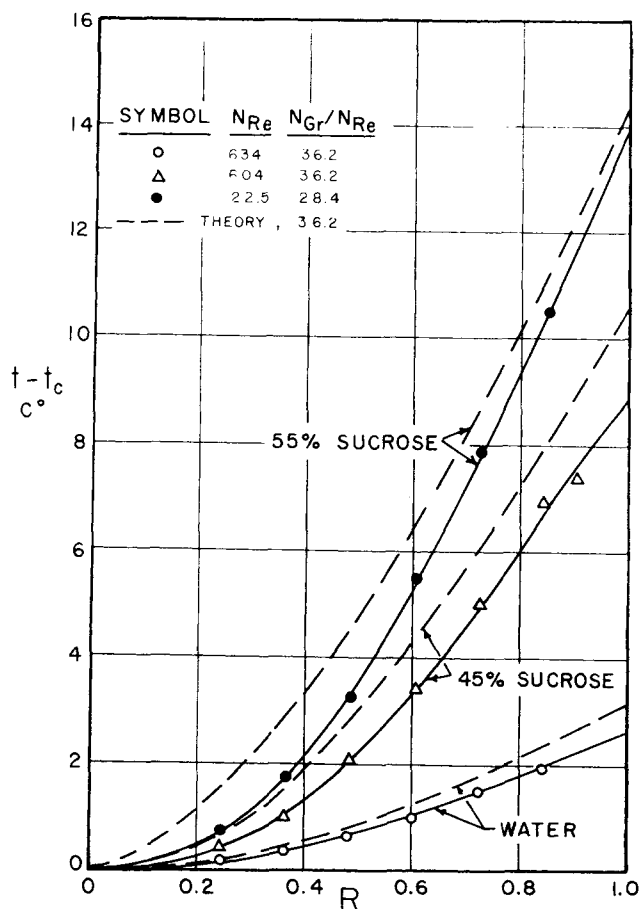


Fig. 7. Temperature profiles for water and sucrose solutions at  $L/D = 251$ .

$N_{Re}$  is increased. Scheele and Hanratty (16) have found that only in very long pipes is a constant limiting value of the critical  $N_{Gr}/N_{Re}$  obtained which is independent of  $N_{Re}$ . They suggest that the dependence of the critical  $N_{Gr}/N_{Re}$  ratio on  $N_{Re}$  arises when the heated length is no longer sufficient for establishment of the least distorted unstable velocity profile and subsequent growth of initially small disturbances.

Scheele and Hanratty found that for heated  $L/D$ 's less than 305, the limiting  $N_{Gr}/N_{Re}$  for water was not obtained for  $N_{Re}$  greater than 100, a result consistent with the present data. They found the lower critical  $N_{Gr}/N_{Re}$  ratio based on outlet temperature to be 42.5. Assuming that this limit is also applicable in the present study, the sucrose solution data indicate that the limiting critical ratio decreases with increasing liquid viscosity. For 45% sucrose the limit appears to be between 36 and the extrapolated value of 29, while for 55% sucrose the limit is between 22 and 16. While the distinction drawn between limiting transition values of  $N_{Gr}/N_{Re}$  for the two sucrose solutions requires data at lower  $N_{Re}$  for confirmation, it seems clear that in both cases the limit is lower than the well-established value previously found for water.

The critical  $N_{Gr}/N_{Re}$  transition ratios for the three fluids suggest the conclusion, previously made on the basis of water results, that the flow is unstable only for velocity profiles having a point of inflection, since the constant viscosity theory predicts the occurrence of such profiles for  $N_{Gr}/N_{Re} > 32.94$ . The decrease in the limiting critical value of  $N_{Gr}/N_{Re}$  with increasing liquid viscosity suggests that the increasing liquid viscosity gradient leads to a greater flow field distortion at a given  $N_{Gr}/N_{Re}$ . This conclusion is consistent with the observed increased distortion of the velocity profiles beyond that predicted by theory and the effect of increasing viscosity on the experimental temperature distributions. From a practical point of view, the data indicate that transition criteria established for low viscosity liquids will be conservative for more viscous liquids (that is, transition occurs at lower  $N_{Gr}/N_{Re}$  ratios) when natural convection is in the direction of the forced flow. Theoretical stability analyses show the importance of velocity profile curvature on flow stability. For example, for nonrotationally symmetric disturbances, Batchelor and Gill (1) and Schade (11) show that the inviscid instability criterion is

$$\frac{d^2U}{dR^2} + \frac{1}{R} \frac{(n^2 - \alpha^2 R^2)}{(n^2 + \alpha^2 R^2)} \frac{dU}{dR} = 0 \quad (11)$$

Therefore, if one wants to use constant heat flux ex-

periments to evaluate stability analyses by comparing experimental results with theoretical predictions, either very low viscosity liquids must be used to minimize radial temperature differences so that the velocity distribution given by Equation (1) is valid, or viscosity effects must be included in the flow field analysis as suggested by Lawrence and Chato (9). Although the Lawrence and Chato analysis is not applicable to the present experiments because of a parabolic rather than uniform velocity distribution at the start of the heat transfer section, a similar analysis is necessary to interpret the present experimental results even for liquids with viscosities as low as that of water.

Even if variable viscosity is included in the analysis, the comparison of theoretical with experimental results may be difficult because the continuously varying distribution makes it difficult to determine the initial unstable experimental velocity distribution (9). Fortunately, for mild heating conditions such as those in the present experiments, the data indicate that even though viscosity variation affects the flow field, essentially invariant distorted profiles should be established downstream in the heat transfer section provided the heated  $L/D$  is sufficiently large, a result not inconsistent with the trend shown by the data of Lawrence and Chato as the radial temperature gradient is decreased.

#### Inception and Growth of Disturbances

The transition process is shown typically in Figures 9 and 10 for water and 45% sucrose, respectively. Each figure shows the temperature behavior as a function of radial position for four axial locations in the heated tube, starting at the  $L/D$  where temperature fluctuations were first detected. This  $L/D$  was always well within the developing flow region. These fluctuations probably first occur at a critical radial location, but because of their initially small amplitude and because the heated length could be varied only in 1 ft. increments, the first detectable fluctuations always occurred within a narrow radial band. As the heated length increases, the fluctuations are seen to grow radially and in amplitude until the entire flow field is disturbed.

The radial location of the initial instability, estimated to be at the midpoint of the range over which disturbances were initially detected, is plotted as a function of outlet  $N_{Gr}/N_{Re}$  in Figure 11. The scatter among these points is most likely caused by inability to observe each unstable temperature profile in precisely the same stage of disturbance growth. Each initial disturbance point in Figure 11 is labeled with the  $L/D$  value at which turbulence was first observed. For any one fluid, the radial location is seen to

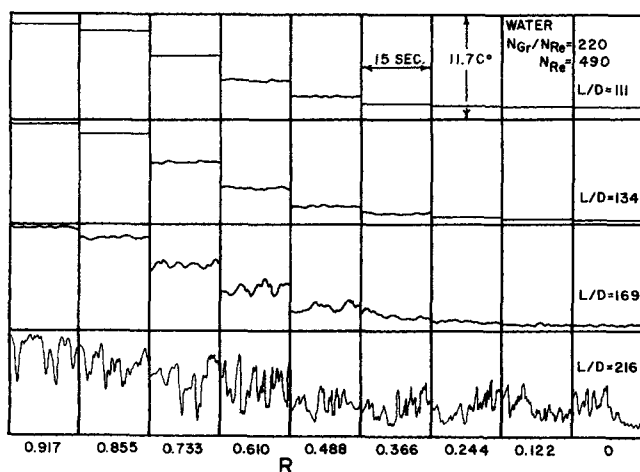


Fig. 9. Growth of disturbances in water.

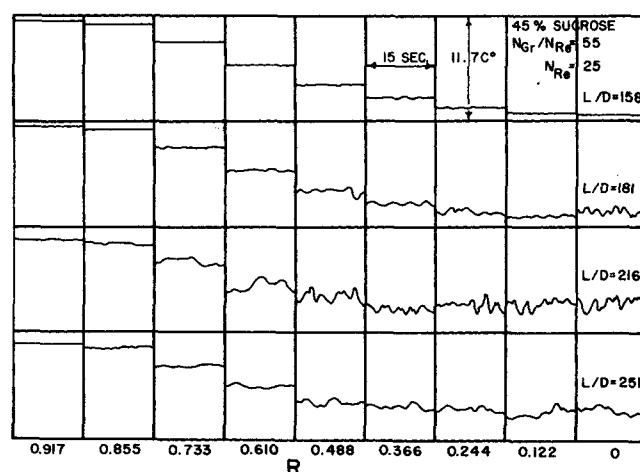


Fig. 10. Growth of disturbances in 45% sucrose solutions.

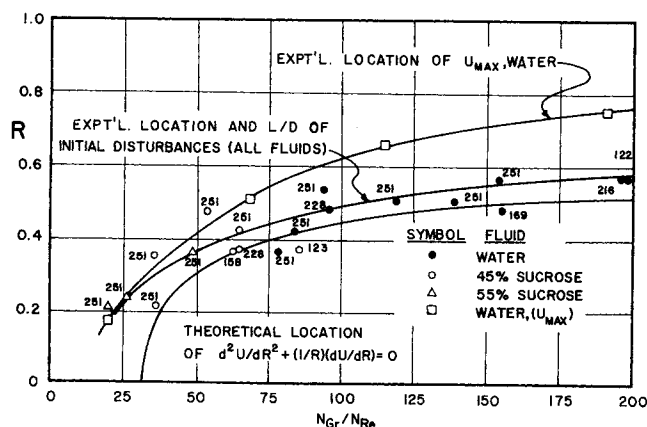


Fig. 11. Radial positions of velocity profile features.

depend on the  $N_{Gr}/N_{Re}$  ratio. For example, for water the critical radius increases from 0.37 at a ratio of 78 to 0.58 at a ratio of 192. In addition, reduction in heated  $L/D$  from 251 to about half this value does not seem to significantly influence the radial location of the initial disturbance for a given  $N_{Gr}/N_{Re}$  as also shown in Figure 11.

It is probable that the radial shift in the initial instability results from the changing shape of the least distorted unstable velocity profile with increasing  $N_{Gr}/N_{Re}$ . Measurements of the developing velocity profiles for water show that their shape is a function of  $N_{Gr}/N_{Re}$ . No conclusions can be drawn regarding the feature of the velocity profiles which leads to instability, since few profile measurements were made at the onset of instability.

However, it is interesting to speculate on the possible profile characteristics responsible for transition. The features of the least distorted unstable velocity profiles are likely to show the same trend with increasing  $N_{Gr}/N_{Re}$  as do the essentially fully developed distorted profiles. Accordingly, Figure 11 also shows the experimental radial location of  $U_{max}$  for fully developed water profiles and the theoretical radial locations of  $U_{max}$  and the position where  $d^2U/dR^2 + (1/R)(dU/dR) = 0$  for velocity distributions described by Equation (1). The latter can be seen from Equation (11) to be inviscid instability criterion for nonrotationally symmetric disturbances as the disturbance wave number approaches zero. Velocity profile measurements were sufficiently imprecise to rule out any attempt to determine experimental locations where  $d^2U/dR^2 + (1/R)(dU/dR) = 0$ .

Because experimental stability results obtained in the developing flow region are being compared with features of fully developed flow, including those predicted by the admittedly approximate constant viscosity theory, quantitative comparisons are meaningless. Of most significance is the fact that the features of the profiles show the same radial trend with increasing  $N_{Gr}/N_{Re}$  as the experimental location of the initial disturbances, supporting the contention that the instability is a function of profile shape. If this is true, there is no reason for all initial disturbance data to fall on the same curve, as suggested in Figure 11, because of the differing effects of viscosity on profile development for the three fluids studied. The results are sufficiently encouraging to justify a thorough study of velocity profiles at incipient transition.

## CONCLUSIONS

1. Measurements of velocity and temperature profiles for constant flux upflow heating of water and temperature profiles for two viscous aqueous sucrose solutions have

been made. At the lowest Reynolds numbers for which velocity profiles could be satisfactorily determined, the profiles did not obtain their maximum distortion within the maximum length of heated pipe available. Experimental evidence suggests that the continuing profile development resulted from insufficient heated  $L/D$  rather than from radial viscosity variations.

2. Nevertheless, small but significant differences between experimental profiles and theoretical velocity profiles based on natural convection effects (neglecting viscosity variations), which can be attributed only to radial viscosity variations with temperature, occur for water with radial temperature differences less than  $2.5^\circ\text{C}$ . The most important is the shift off center of the maximum velocity at lower  $N_{Gr}/N_{Re}$  ratios than predicted. Thus viscosity effects can influence distorted velocity profiles for laminar upflow constant flux heating even for relatively nonviscous liquids and mild heating conditions.

3. Both experimental velocity and temperature profiles at considerably larger heated  $L/D$ 's or smaller  $N_{Re}$  are necessary to determine the extent of viscosity vs. profile development effects under various heating and flow conditions. An improved technique must be developed.

4. Sufficient distortion of the velocity profile will induce transition to disturbed flow at low  $N_{Re}$ . The limiting  $N_{Gr}/N_{Re}$  transition ratio decreases as the radial viscosity variation increases. The experimental transition ratios indicate that the flow is unstable only for velocity profiles in which the maximum velocity has moved off center. Experimental velocity measurements for liquids more viscous than water will be necessary to confirm this conclusion.

5. An adaptation of the variable density and viscosity analysis of Lawrence and Chato to an initially parabolic velocity distribution will be necessary to compare experimental transition results with stability theory predictions. The constant viscosity analysis is clearly inadequate. Still undetermined is the question of whether the profiles become essentially invariant.

6. The location both radially and axially of the initial instability depends on the critical value of  $N_{Gr}/N_{Re}$ . The instability grows both radially and in amplitude with increasing heated length. The experimental radial location of the initial disturbance is in fairly good agreement with that predicted by the inviscid instability criterion for small wave number disturbances which requires that  $d^2U/dR^2 + (1/R)(dU/dR) = 0$  at the radial position of instability.

## NOTATION

- $a$  = pipe radius
- $bei(x)$  = imaginary part of  $I_0(\sqrt{i}x)$
- $ber(x)$  = real part of  $I_0(\sqrt{i}x)$
- $C_p$  = heat capacity at constant pressure
- $D$  = pipe diameter
- $g$  = acceleration of gravity
- $h$  = local film heat transfer coefficient
- $I_0(x)$  = modified Bessel function of first kind of order zero
- $k$  = liquid thermal conductivity
- $L$  = heated length of pipe
- $n$  = disturbance parameter, 0 for rotationally symmetric disturbances
- $N_{Gr}$  = modified Grashof number,  $a^4\rho^2g\beta q/k\mu^2$
- $N_{Nu}$  = Nusselt number,  $hD/k$
- $N_{Pr}$  = Prandtl number,  $C_p\mu/k$
- $N_{Ra}$  = Rayleigh number,  $(N_{Gr}/N_{Pr})$
- $N_{Re}$  = Reynolds number,  $aU_{avg}\rho/\mu$
- $q$  = heat flux
- $r$  = radial position coordinate
- $R$  = dimensionless radius,  $r/a$



$t$  = local temperature  
 $T$  = dimensionless temperature,  $t_w - t/t_w - t_c$   
 $u$  = local axial velocity  
 $U$  = dimensionless velocity,  $u/U_c$   
 $U_{avg}$  = average fluid velocity in axial direction  
 $U_c$  = fluid velocity at pipe center in axial direction  
 $U_{max}$  = maximum local velocity in axial direction  
 $\alpha$  = disturbance wave number  
 $\beta$  = coefficient of volumetric expansion  
 $\mu$  = liquid viscosity  
 $\rho$  = liquid density  
 $c$  = quantity evaluated at  $R = 0$   
 $w$  = quantity evaluated at  $R = 1$

#### LITERATURE CITED

1. Batchelor, G. K., and A. E. Gill, *J. Fluid Mech.*, **14**, 529 (1962).
2. Brown, C. K., and W. H. Gauvin, *Can. J. Chem. Eng.*, **43**, 306, 313 (1965).
3. Brown, W. G., *VDI Forschungsheft*, No. 480 (1960).
4. DeYoung, S. H., and G. F. Scheele, *AIChE J.*, **16**, No. 5, 712 (1970).
5. Greene, H. L., *Chem. Eng.*, **73**, 22 (1966).
6. Hallman, T. M., *Trans. Am. Soc. Mech. Engrs.*, **78**, 1831 (1956).
7. ———, *N.A.S.A. Tech. Note D-1104* (1961).
8. Hanratty, T. J., E. M. Rosen, and R. L. Kabel, *Ind. Eng. Chem.*, **50**, 815 (1958).
9. Lawrence, W. T., and J. C. Chato, *Trans. Am. Soc. Mech. Engrs. J. Heat Transfer*, **88**, 214 (1966).
10. Metais, B., and E. R. G. Eckert, *ibid.*, **86**, 295 (1964).
11. Morton, B. R., *J. Fluid Mech.*, **8**, 227 (1960).
12. Ostroumov, G. A., *N.A.C.A. Tech. Translation TM 1407* (1958).
13. Pai, S. I., *Report R62SD75*, Space Sciences Laboratory, General Electric (1962).
14. Schade, H., *ASTIA Rept. AD 608096*.
15. Scheele, G. F., and H. L. Greene, *AIChE J.*, **12**, 737 (1966).
16. Scheele, G. F., and T. J. Hanratty, *J. Fluid Mech.*, **14**, 244 (1962).
17. Scheele, G. F., E. M. Rosen, and T. J. Hanratty, *Can. J. Chem. Eng.*, **38**, 67 (1960).
18. Scheele, G. F., unpublished results.
19. Williams, D. B., M.S. thesis, Cornell Univ., Ithaca, N. Y. (1969).

Manuscript received February 1, 1968; revision received April 3, 1969;  
 paper accepted April 7, 1969.

# Compressibilities and Virial Coefficients for Methane, Ethylene, and Their Mixtures

ROY C. LEE and WAYNE C. EDMISTER

Oklahoma State University, Stillwater, Oklahoma

A Burnett type of apparatus was built for 12,000 lb./sq.in. pressure and temperatures of 25° to 100°C. Isothermal expansions were run on methane, ethylene, and four binary mixtures at 25°, 50°, and 75°C., and compressibility factors were derived from the pressure ratio observations.

From the experimental data, second and third virial coefficients were derived by two techniques, that is, the slope-intercept and the multiple regressions curve-fit of the data by the density-series virial equation. A comparison of these virial coefficients with those from the different empirical equations of state indicates areas of needed improvements in these equations. Second virial cross coefficients were also obtained.

Compressibility measurements are of great value in providing needed volumetric data for process design calculations and the derivation of thermodynamic properties, such as enthalpy, entropy, and fugacity. In addition to tabulations, analytical formulations (that is, equations of state) are used in presenting real fluid compressibility factors. The purpose of this work is to contribute useful data and correlations of these kinds.

R. C. Lee is presently at Phillips Petroleum Company, Bartlesville, Oklahoma.

The binary system of methane and ethylene was selected for this study. The compressibility factors for methane, ranging from -274° to 650°F. and from atmospheric pressure to 1,000 atm., have been reported by many investigators (6, 9, 12, 13, 17, 19, 23 to 26, 28, 32). Most of the data are for temperatures above ambient. The volumetric properties of ethylene have not been studied as extensively as methane, covering temperatures from -140° to 500°F. and pressures to 3,000 atm., with most of the data above ambient temperatures (5, 18, 19, 21, 22, 27,